

Guidelines for simulating cryogenic film boiling using volume of fluid (VOF) method

Monir Ahammad^{1†}, Tomasz Olewski², Yi Liu¹, Samina Rahmani¹, Sam Mannan¹ and Luc Vechot^{2*}
Mary Kay O'Connor Process Safety Center

¹Artie McFerrin Department of Chemical Engineering, Texas A&M University, College Station, Texas 77840

² Department of Chemical Engineering, Texas A&M University at Qatar, Doha

†Presenter E-mail: monir@tamu.edu

* Corresponding author: luc.vechot@qatar.tamu.edu

The quality of a risk assessment performed in the context of the cryogenic liquid spills (e.g., LNG) depends on the accurate estimation of the vapor formation due to heat transfer from the ground. During an accidental spill, cryogenic liquids undergo different boiling regimes, from initial film boiling to nucleate boiling via a short living transition regime. At the early stage of the spill, the temperature difference between the liquid and the ground is relatively large; therefore the boiling is expected to fall in the film boiling regime. Thus for an accurate estimation of spill consequences and the simulation of pool spreading, film boiling simulation for cryogenic liquid is very important but unfortunately not trivial. This paper discusses the use of computational fluid dynamic (CFD) approach for the simulation of film boiling of a cryogenic liquid and provides a general guideline to simulate film boiling using a commercial CFD software package ANSYS-FLUENT.

Keywords: LNG spill, source term modelling, cryogenic liquid boiling, volume of fluid, CFD

1 Introduction

The world demand of Liquefied Natural Gas (LNG) has significantly increased in recent years. Extremely large quantities of LNG are being handled every day to meet the increased fuel demand around the globe. Accidental loss of containment of LNG storage tanks or leak in the complex processing plants may lead to disastrous consequences. Accurate consequence modeling is therefore of central importance for the assessment of the risks associated to LNG facilities and to prevent incidents, mitigate the consequences and plan for emergency responses.

LNG safety dedicated literature sources show that extensive research has been focused on vapor dispersion calculation, a part of consequence analysis, whereas, source term modeling, *i.e.* prediction of the vapor production rate has received much less attention (Webber et al. 2010). Source term models provide the input data to dispersion models, thus, if the source term is not accurately assessed, the dispersion calculation and the subsequent risk assessment will be flawed.

In case of cryogenic liquid spills on ground, the source terms include the liquid discharge from the primary containment, flashing, droplets formation, rain-out, pool formation, pool spread and heat transfer to the pool from the surrounding. These are the different aspects of source term modeling that govern the vapor formation from accidental spill that may occur through boiling or evaporation. This paper focuses on heat transfer to a cryogenic liquid pool from a solid ground.

In the particular case of a cryogenic liquid spill on ground, the vaporization rate of the cryogenic liquid pool is dominated by the heat transfer from the ground, at least at the early stages of the spill (Véchet et al. 2013). The large temperature difference between the ground and the liquid generates vigorous boiling. The liquid pool can undergo different boiling regimes, from film boiling to nucleate boiling (Figure 1). Heat transfer correlations are mainly used to describe the heat transfer in these regimes; however the correlations are limited by many assumptions, lack of validations and cannot capture the dynamic nature of boiling.

Computational Fluid Dynamics (CFD) is recognized as a very promising tool for this application. However, it presents very significant challenges and costs. This work discusses the use of CFD to model the boiling of a cryogenic liquid on a solid substrate during the film boiling regime. The ANSYS-FLUENT a commercial software package was used in this work. The key parameters in CFD simulation of film boiling utilizing the Volume of Fluid (VOF) method were identified and a sensitivity analysis of the simulation results performed. This paper provides a general guideline to simulate film boiling using CFD.

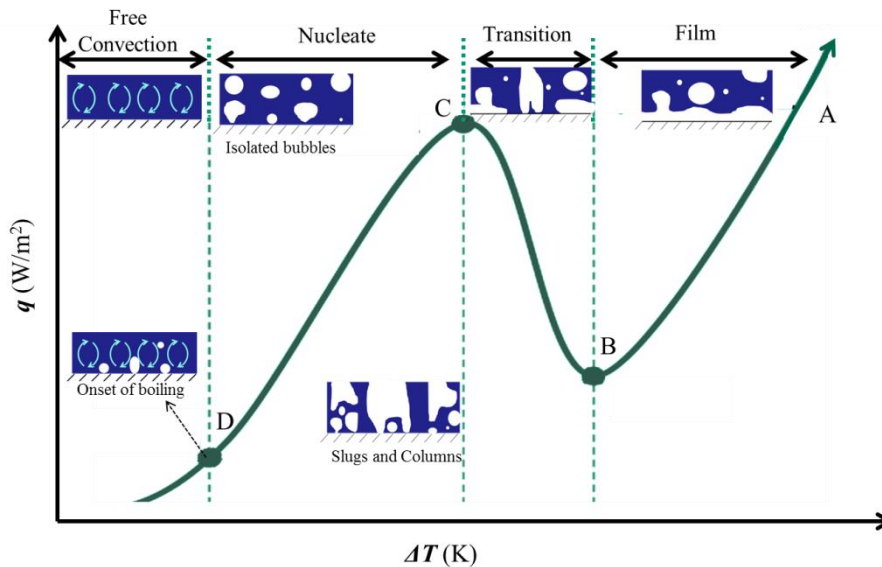


Figure 1: Boiling regimes. A-B: film Boiling, B: Leidenfrost point, B-C: Transition Boiling, C: Critical Boiling Point, C-D: Nucleate boiling and D: Onset of boiling point.

2 Literature Review

Film boiling is characterized by the presence of a continuous vapor film between the hot surface and boiling cryogenic liquid. Two types of modeling approaches are available in the literatures, namely heat transfer correlations and CFD based models. Though CFD model gives more accurate estimation of heat transfer, the heat transfer correlations laid the fundamental framework. The fundamental works are reviewed in this section.

2.1 Heat Transfer Correlations

In a horizontal system where the dense phase lays over the light phase, the interface is stable unless a perturbation causes the instability. This phenomenon is known as Rayleigh-Taylor (R-T) instability. Zuber, 1959 first used the concept of R-T hydrodynamic instability to predict film boiling. The bubble generation due to film boiling is also an R-T instability phenomenon. During this types of phenomena where the interface rises against the gravity, the surface tension and gravity acts to stabilize the interface perturbation. Two fundamental dimensions namely “critical wavelength” and “most dangerous wavelength” were also introduced from the study of Zuber, 1959:

- The “critical wavelength” is defined as the minimum wavelength of perturbation/disturbance below which the interface will not grow or rise. In another words, the film will be sustained without any bubble generation. Carey (Carey 1992) used perturbation analysis to show that the critical wavelength is

$$\lambda_c = 2\pi \left[\frac{\sigma}{(\rho_l - \rho_v)g} \right]^{1/2} \quad (1)$$

- The “most dangerous wavelength” is defined as the disturbance wavelength for which the maximum number of bubbles will grow. This is defined as follows:

$$\lambda_{d2} = 2\pi \left[\frac{3\sigma}{(\rho_l - \rho_v)g} \right]^{1/2} \quad (2)$$

Zuber, 1959 suggested that for bubbles generating from a flat plate, the nearest distance of two rising bubbles from a continuous film is bounded by “critical” and “most dangerous” wavelength of R-T instability. He also assumed the release of two bubbles per cycle from a square cell and used this assumption to calculate the minimum heat flux at Leidenfrost point.

Further extending this concept, Berenson, 1961 derived the expression for calculating heat transfer coefficient from a substrate to a liquid during a saturated film boiling on flat surfaces. His static model assumed bubble placement on a square grid spaced by a distance of “most dangerous” Taylor wavelength on thin film of vapor.

The two-dimensional configuration study of Zuber and Berenson was improved for three dimensions by Sernas *et al.*, 1973. They showed that three dimensional Taylor wavelength, λ_{d3} is $\sqrt{2}$ times larger and release four bubbles per cycle from an λ^2 area.

Klimenko, 1981 attempted to generalize the film boiling correlation on horizontal flat plates for different liquids including cryogenics. However, heat transfer correlations also known as static models do not capture the dynamic nature of interface variation. Hence correlations cannot predict the temporal variation of heat flux which is directly affected by the temporal variations of vapor-liquid interfaces. Therefore, CFD simulation of film boiling is used to estimate the dynamic nature of bubbles growing from the vapor film and to accurately estimate the heat-flux *i.e.*, the rate of boiling.

2.2 CFD based Modeling

For an accurate determination of the boil-up rate of cryogenic liquid such as LNG, the transient and dynamic aspects of boiling need to be studied properly. With the advances in high performance computation capability, CFD simulation of complex problem such as film boiling is rendered possible.

CFD simulation of horizontal film boiling has been pioneered by Son and Dhir, 1997 who studied bubble and film dynamics for water boiling using a moving-mesh method. Banerjee and Dhir, 2001, simulated sub-cooled film boiling of water on a horizontal disk. Dhir, 2001 presented a combined nucleate and film boiling scheme and simulated for water. Juric and Tryggvason, 1998, used added interfacial source terms in the continuity equations on an Eulerian grid to simulate horizontal film boiling of low density ratio fluid to high density ratio fluid. This numerical method was further improved by Esmaeeli and Tryggvason, 2004 by elimination of iterative algorithm. Son and Dhir, 1998 simulated axisymmetric horizontal film boiling for water near critical conditions and provided steady-state periodic bubble release pattern. Welch and Wilson, 2000 used Youngs, 1982 Volume of Fluid (VOF) method to simulate saturated horizontal film boiling including conjugate heat transfer from the wall. Using this method, Welch and Rachidi, 2002, simulated film boiling of water in contact with steel. Yuan *et al.*, 2008 simulated the film boiling of water on a sphere on a non-orthogonal body fitted coordinates.

Liu *et al.*, 2011, studied pool boiling of liquid nitrogen using commercial computational fluid dynamics package ANSYS-Fluent. He attempted to predict the heat flux in the different boiling regimes using a film boiling simulation approach combined with a source term as defined in Equation 6. It is shown that the simulated data predict well the experimental data (Merte and Clark 1964) in the film boiling regime. However, this study does not use the “*most dangerous*” wavelength for film boiling simulation. The experimental data that were used to compare (Merte and Clark 1964) describes a quenching experiment of a copper sphere. The simulation was conducted for flat plate film boiling and was compared against the film boiling on from a sphere surface. Thus the result is not coherently compared. Furthermore, the addition of previously mentioned source term which is essentially an evaporation model may not represent an actual boiling case. In addition to that, no useful guideline is available in selecting the right parameter while performing CFD simulations of film boiling.

In short, several authors employed numerical simulations as a tool to model film boiling in the last decade, no attempt have been taken to simulate cryogenic fluid except Liu *et al.*, 2011. Additionally, most of the studies refer to boiling systems involving water and refrigerants. The setting-up of the film boiling simulation for cryogenics are not trivial because of the extreme values of dimensionless parameters that are linked to cryogenic temperatures. Thus, the objective of this study is to systemically analyze different parameters of commercial CFD package Fluent in order to provide a general guideline for users.

3 Film Boiling Simulations using CFD

In this work, commercial CFD package ANSYS-FLUENT is used to simulate liquid film boiling. Figure 2, presents the general idea of film boiling simulations used in this study. It is assumed that the substrate roughness is much smaller than the film thickness and the bubble evolves in a regular pattern from the film. One bubble evolves in each cycle from a square cell of area $\lambda_{d2}^2/4$, where λ_{d2} is the “*most dangerous*” Taylor wavelength. The point at which bubbles is growing is referred to as *node* and the valley of two adjacent bubbles is named *antinode*. Considering the symmetry of the bubbles over the entire heated surface, a horizontal length of $\lambda_{d2}/2$ is needed to be simulated. To capture the bubble dynamics properly, the height of the two-dimensional simulation region should be at least three times higher than its width (Ansys *Inc.* 2011). The bottom of the domain is considered as a “hot” surface at given constant temperature whereas the top of the domain is considered as the outlet for the vapor generated due to boiling and hence vapor outlet. The sides of the domain are considered symmetry. Mirror imaging of the simulated grid will result in bubble dynamics of a cell. The computational grid of $\lambda_{d2}/2$ in length is divided into 64 cells in the horizontal direction and $3\lambda_{d2}/2$ of height is divided in 192 cells in the vertical direction. Volume of Fluid (VOF) method is used to track the interface phenomena.

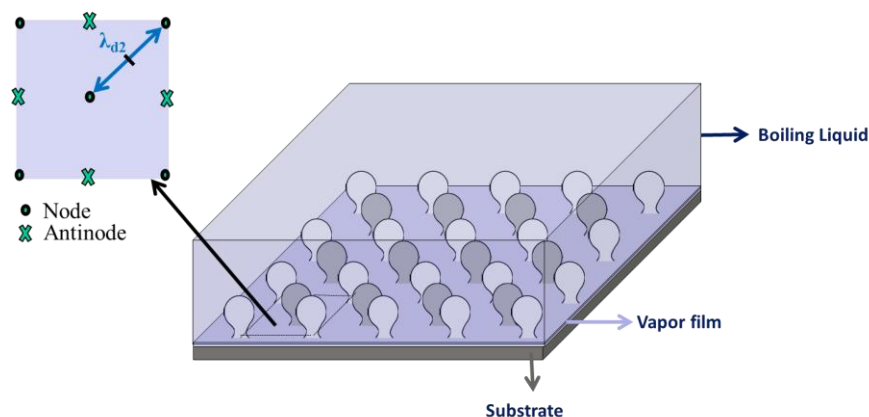


Figure 2: R-T instability wavelength and film boiling simulation approach.

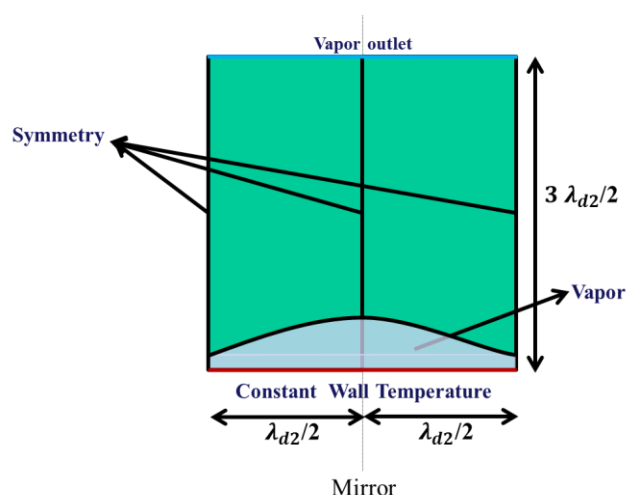


Figure 3: Setup of 2D film boiling simulation.

To initialize the film boiling simulation, a film of vapor at the bottom of the computational grid is generated manually. R-T instability is given as function of sinusoid perturbation in the vapor liquid interface as defined by Equation (3).

$$\delta = \frac{\lambda_{d2}}{64} \left(4 + \cos\left(\frac{2\pi x}{\lambda_{d2}}\right) \right) \tag{3}$$

This computational technique is also used in ANSYS-Fluent tutorial (Ansys Inc. 2011) to demonstrate the film boiling simulations of a hypothetical fluid with a boiling point of 500K and 10K wall superheat. Later in this paper we call this methodology, base case. However, our effort of applying the same methodology to cryogenic fluids such as Liquid Nitrogen, Liquid Methane was unsuccessful. As shown in Figure 4, the initial vapor film contracts to the node and eventually the domain becomes vapor free with time, thus the film boiling simulation is not possible. Perhaps, the extreme values of the crucial parameters such as surface tension at cryogenic conditions might be linked to difficulty of simulating film boiling. On the other hand, Liu *et al.*, 2011 successfully simulated cryogenic boiling using the same approach, however no guideline was given on how they came to all settings and how to set a critical parameters and which are significant. Later in this paper we call Liu *et al.*, 2011 setup a working case. In this paper, we study all potentially significant parameter separately and give a guideline on which parameters or setups are necessary and which are significant. The success of film boiling is determined by the persistent vapor film at the bottom and generation of bubble cycles for a sufficiently large time such as 3 seconds. The difference between the setup of the base case and the working case is presented in Table 1. Starting from the base case, a series of simulations has been completed in order to establish the complete guideline.

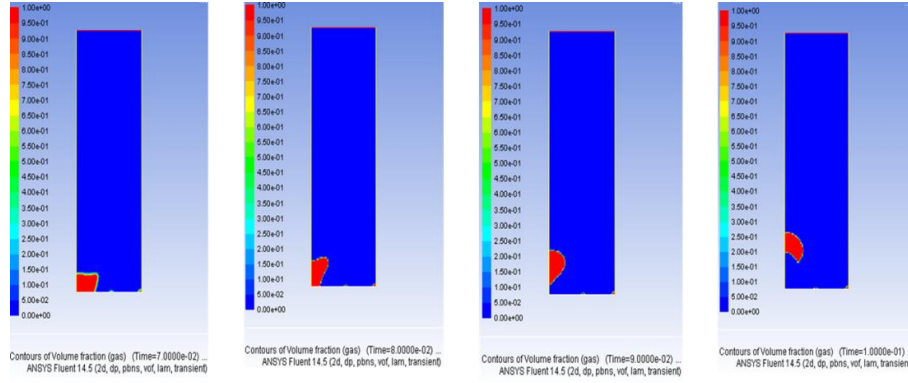


Figure 4: Film boiling simulation of liquid nitrogen while following the base case for wall superheat of 35K (Mirror reflection is not shown here).

Table 1: Difference between the base case (Ansys Inc. 2011) and working case (Liu *et al.* 2011).

	Baseline	Working case
Length scale	$\lambda_{d2} = 2\pi \left(\frac{3\sigma}{(\rho_l - \rho_g)g} \right)^{0.5}$	$\lambda_{d2} = 2\pi \left(\frac{2\sigma}{(\rho_l - \rho_g)g} \right)^{0.5}$ (4)
Material property ($\rho, C_p, k, \mu, \sigma$)	Constant	Temperature Dependent
Phase interaction	CSF	CSF + Eva – Cond model (freq = 0.00385, $T^{sat} = 77K$)
Operating Conditions	Density = 4.5 kg/m ³	Density = 807.3 kg/m ³
Wall BCs	No-slip Backflow T = 77K Liquid backflow	Marangoni Stress ($\frac{\partial\sigma}{\partial T} = -0.00028$) Backflow T = 273 K Vapor backflow
Initialization	Linear T Gradient	$T_y = \rho_{cell} \times y$ (5)
Heat Transfer Source Term	At Interface	Additional Source 2 in UDF:

The length scale used in the base case is essentially the “most dangerous” Taylor wavelength also used in other literatures (Banerjee and Dhir 2001; Son and Dhir 1998; Dhir 2001). However, the working case uses a different definition which was believed to generate maximum amount of vapor (Tomar *et al.* 2005). At the cryogenic temperatures, a small change in temperature can cause large variation of the thermodynamic properties of the fluid. A Continuum Surface Force (CSF) model of surface tension force modelled by Brackbill, Kothe, and Zemach, 1992 is used for surface tension which plays very important role in the interface dynamics. In the working case model, Lee’s Evaporation – Condensation (Eva-Cond) model (Ansys Inc. 2013) is also used to fit experimental results. Base case suggests using the vapor density as the operating condition whereas the density of liquid is used in the working case. For the wall Boundary conditions (BCs) no-slip conditions is used whereas Marangoni stress (Juric and Tryggvason 1998) is used in the working case. The backflow temperature of the vapor was also assumed differently. Consideration of the backflow phase is crucial in the convergence of the problem. Finally, in the base case – interfacial heat transfer is modelled using the following formula:

$$S_{\alpha,L} = \frac{(q_l - q_v)\nabla\alpha}{L_v} \quad (6)$$

whereas, in the working case an additional source term with the interfacial heat transfer term is added for the consideration of homogeneous boiling. The additional source term which is referred as source 2 is defined as follows:

$$S_{g,2} = \frac{Q_2}{L_v} = \frac{\alpha_l \rho_l C_{p,l} (T_l - T_{sat})}{L_v \tau} \quad (7)$$

4 Guideline Formulations

A step by step change in the simulation parameters that are used to develop this guideline is presented in the following table.

Table 2: Table of simulated cases

Simulation no	Parameter changed from base case	Parameter used in simulated case	Successful?
1	Length scale as Equation (2)	Length scale as Equation (4)	No
2	Constant ρ, C_p, k, μ	$\rho(T), C_p(T), k(T), \mu(T)$	No
3	Constant ρ, C_p, k, μ and length scale as Equation (2)	$\rho(T), C_p(T), k(T), \mu(T)$ and length scale as Equation (4)	No
4	Constant ρ, C_p, k, μ and CSF	$\rho(T), C_p(T), k(T), \mu(T)$, CSF and Eva - Cond model	No
5	Constant ρ, C_p, k, μ , and liquid back flow	$\rho(T), C_p(T), k(T), \mu(T)$, and vapor backflow	No
6	Constant $\rho, C_p, k, \mu, \sigma$ and no-slip at wall BC	$\rho(T), C_p(T), k(T), \mu(T), \sigma(T)$ and Marangoni stress at wall	No
7	Constant ρ, C_p, k, μ and specified operating density for vapor	$\rho(T), C_p(T), k(T), \mu(T)$, and specified operating density for liquid	No
8	Constant ρ, C_p, k, μ , length scale as Equation (2) and liquid back flow.	$\rho(T), C_p(T), k(T), \mu(T)$, length scale as Equation (4) and vapor backflow.	No
9	Constant ρ, C_p, k, μ , length scale as Equation (2) and specified operating density.	$\rho(T), C_p(T), k(T), \mu(T)$, length scale as Equation (4), and specified operating density for liquid	No
10	Constant $\rho, C_p, k, \mu, \sigma$, length scale as Equation (2) and no-slip at wall BC.	$\rho(T), C_p(T), k(T), \mu(T), \sigma(T)$, length scale as Equation (2), and Marangoni stress at wall	No
11	Constant $\rho, C_p, k, \mu, \sigma$, length scale as Equation (2), no-slip at wall BC and linear T gradient	$\rho(T), C_p(T), k(T), \mu(T), \sigma(T)$, length scale as Equation (4), Marangoni stress at wall and T initialization as Equation (5).	Yes
12	Constant $\rho, C_p, k, \mu, \sigma$, length scale as Equation (2) no-slip at wall BC and linear T gradient	$\rho(T), C_p(T), k(T), \mu(T), \sigma(T)$, length scale as Equation (2), Marangoni stress at wall and initialization as Equation (8).	Yes
13	Constant $\rho, C_p, k, \mu, \sigma$, length scale as Equation (2), no-slip at wall BC and Linear T Gradient	$\rho(T), C_p(T), k(T), \mu(T), \sigma(T)$, length scale as Equation (2), Marangoni stress at wall and initialization as Equation (8).	Yes
14	Constant $\rho, C_p, k, \mu, \sigma$, length scale as Equation (2), and Linear T gradient	$\rho(T), C_p(T), k(T), \mu(T), \sigma(T)$, length scale as Equation (2) and T initialization as Equation (8).	No
15	Constant σ , length scale as Equation (2), no-slip at wall BC and initialization	$\sigma(T)$, length scale as Equation (2), Marangoni stress at wall and initialization as Equation (8).	Yes
16	Constant $\rho, C_p, k, \mu, \sigma$, length scale as Equation (2), no-slip at wall BC, Linear T Gradient and vapor backflow	$\rho(T), C_p(T), k(T), \mu(T), \sigma(T)$, length scale defined as Equation (2), Marangoni stress at wall, T initialization as Equation (8) and liquid backflow.	Diverged after the first bubble generation.
17	Constant $\rho, C_p, k, \mu, \sigma$, length scale as Equation (2), no-slip at wall BC, initialization and specified operating density for vapor	$\rho(T), C_p(T), k(T), \mu(T), \sigma(T)$ length scale as Equation (2), Marangoni stress at wall, T initialization as Equation (8) and specified operating density for liquid	Yes

In simulation 1, the length scale of the base case as defined by Equation (2) is changed to Equation (4) by keeping all other parameters constant. Change of length scale changes the computational domain as discussed in the previous section. The initial perturbation function as shown in Equation (3) was also adjusted accordingly. However, it did not result success. In the simulation 2, the physical property of both phases has changed to piece wise linear temperature dependent function (Rowley *et al.* 2003). Then, for simulation 3 to 7, parameters such as length scale, CSF, liquid backflow, no-slip condition at wall and specified operating density are changed consecutively to length scale defined by Equation (4), CSF + Eva-Cond model, specified operating density for liquid, Marangoni stress condition at wall and CSF with evaporation condensation model were used. However, simultaneous change in two parameters for these cases does not result in a successful simulation. For the simulation 8, 9 and 10, three parameters i.e., physical properties of both phases, wall slip condition and back flow condition has been changed

simultaneously for the length scale defined by Equation (4). Even for these cases, the film boiling simulations were not successful. Finally for the simulation 11, when the initial temperature of the domain has changed to the equation (5), a successful film boiling simulation for liquid nitrogen has been observed. It is to be noted that, in the base case initialization procedure, a linear temperature gradient has been applied from the wall to the outlet irrespective of the phase condition (*i.e.*, vapor of liquid). Furthermore, the initial temperature of the computational nodes as defined by Equation (5) does not carry meaningful information. Therefore, a more physical meaningful temperature initialization condition is suggested as below:

$$T_y = \begin{cases} T_{wall} - \Delta T \cdot y/\delta & \text{for } \alpha = 1 \\ T^{sat} & \text{for } \alpha = 0 \end{cases} \quad (8)$$

Equation (8) describes a linear temperature profile in the initial vapor film whereas the temperature of the liquid is at its boiling point. This change is adapted in simulation 12 and successfully simulated. To investigate the dependency of length scale, the length scale as defined by Equation (2) is used in the simulation 13. It was found that it is possible to simulate film boiling by using “most dangerous” wavelength. As literature suggests (Carey 1992), this would generate the maximum vapor generation. In simulation 14, the necessity of Marangoni wall condition has been investigated by restoring this condition to no-slip condition. However, it turned out to be a necessary condition to be able to simulate the film boiling. Simulation 15 investigated which physical property plays the most important role. Thus one by one, density, viscosity, thermal conductivity and surface tension have been changed from base case and it is observed that the surface tension plays the most important roles in film boiling simulation. Using temperature dependent surface tension and constant other physical properties, it is possible to simulate cryogenic film boiling. In simulation 16, the effect of vapor backflow has been investigated. The simulation diverges when the first bubble rises to the outlet of the computational domain. The possible explanation of this event is, while the bubble leaves the domain, equivalent amount of liquid backflows and results in much turbulence that the solution methods cannot handle. This problem has been solved by repeating this simulation using a vapor backflow. Finally, simulation 17 was used to investigate the effect of specified operating density of the computational domain. The base case uses the density of vapor whereas the working case uses the density of liquid. However, it is observed that, by allowing sufficient number of iterations for each time step, this parameter does not affect the film boiling simulation. Figure 1, depicts a typical successful simulation where continuous bubble generates from the vapor film during LN2 boiling at a wall superheat of 35K.

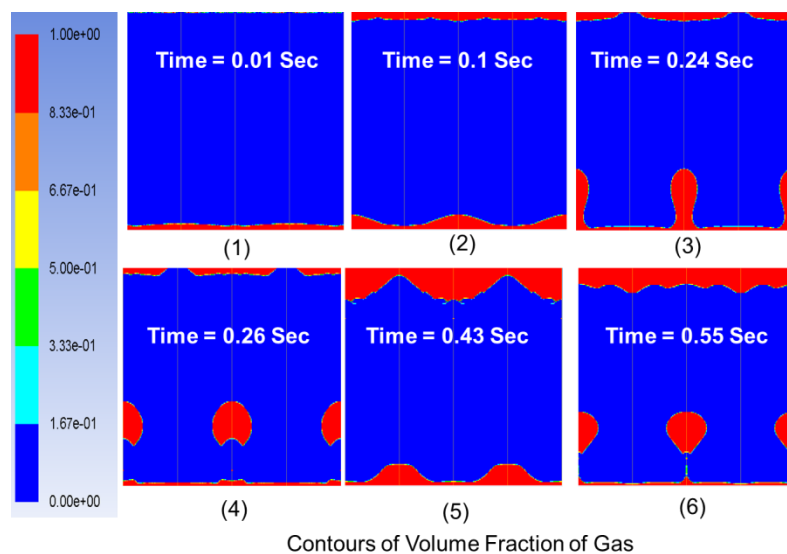


Figure 5: A typical successful simulation. Figure shows bubble generation during film boiling of Liquid Nitrogen at wall temperature of 150K.

5 Recommendations

The result of the series of simulations as discussed in the previous section can be used as a general guideline to be followed while setting up film boiling simulations for cryogenic fluids. The recommendations of this study are as follows:

- While setting up film boiling simulation using the above mentioned approach, among the physical properties, at minimum the surface tension of the cryogenic fluid should be considered as temperature dependent property. In this concept of film boiling simulations, the surface tension and gravity tries to stabilizes the initial perturbation and since surface tension significant varies with small temperature change it is a necessary condition. For accurate computations, other thermodynamic properties can also be considered as temperature dependent.

- Marangoni stress at the wall owing to the surface tension variation in the vapor film needs to be considered instead of no-slip condition at wall.
- Backflow phase can affect the computational stability of the simulation. If the backflow is considered as liquid while the flow condition is set to laminar in the computational domain, it can induce significant turbulence and make the problem difficult to converge. On the other hand, considering a vapor backflow at boiling point will not induce turbulence.
- The proper initialization of temperature in the computation domain is extremely important. The following base case can be misleading. A sensible way of assigning temperature in the domain could be setting the temperature at the liquid boiling point and imposing a linear temperature gradient inside the vapor film. This approach has been found to provide the best results.
- The choice of the transient time step should be such that the Courant-Friedrichs-Lewy (CFL) number should always remain less than 1. Good engineering judgment should be used in the selection of time step so that the simulation speed is not compromised to ensure numerical stability.
- The length scale of the simulation does not affect the success of R-T instability simulation. However, it is fundamental in setting up the problem.
- Lees Evaporation-Condensation model and additional “source 2” of Liu *et al.* 2011 are the same model but expressed differently. It is not necessary to use additional source term to successfully simulate film boiling.
- Finally, the operating density or the selection of primary fluid does not affect the success of film boiling simulation as it just provides the starting value in an iterative algorithm of Navier-Stokes system of equation.

6 Conclusions

The theoretical background for CFD simulation of cryogenic film boiling was presented in this paper. Because of the extreme values of the thermodynamic properties of the liquid at cryogenic temperature, it is not trivial to simulate film boiling. Therefore, a comprehensive literature review was conducted to establish a basis for determining the important parameters for the simulation of film boiling for cryogenic fluids. Two references from the literature were respectively considered as the base case (ANSYS tutorial (Ansys Inc. 2011)) and the working case (Liu *et al.* 2011). The differences in the parameters chosen to setup the problem in CFD for both cases were presented. A series of 17 simulations was conducted to determine the most important parameters for the successful set up of a film boiling simulations for cryogenic fluid in CFD. It was found that the surface tension, Marangoni stress, temperature initialization in the computational domain, backflow fluid phase and transient time step are the most important parameters to be considered.

Acknowledgments

This publication was made possible by the NPRP award [NPRP 6-425-2-172] from the Qatar National Research Fund (a member of The Qatar Foundation). The statements made herein are solely the responsibility of the author[s].

Nomenclature

ΔT - Wall super heat (K)

q_w - wall heat flux (W/m².K)

q_l - Heat flux from liquid phase to vapor (W/m².K)

q_v - Heat flux from vapor phase to liquid (W/m².K)

λ - Wave length (m)

λ_c - Critical Wavelength, (m)

λ_{d2} - Two dimensional most dangerous wavelength (m)

λ_{d3} - Three dimensional most dangerous wavelength (m)

σ - Surface tension (N/m)

$\rho_l, \rho_g, \rho_{cell}$ - Density of liquid, vapor and the control volume cell (Kg/m³)

g - Gravitational acceleration, 9.81 (m/s²)

α – Vapor volume fraction
 α_l – Volume fraction of liquid phase
 L_v – Latent heat of vaporization, (J/Kg)
 $C_{p,l}$ – Heat capacity of liquid phase (J/Kg/K)
 T_l – Temperature of liquid phase (K)
 T^{sat} – Saturation temperature (K)
 T_y – Temperature of the cell at the height of y (K)
 x, y – Horizontal and vertical distances of the control volume from the node (m)
 τ – Relaxation time
 δ – Film thickness (m)

References

- Ansys Inc. 2011. “Horizontal Film Boiling (Tutorial),” 1–20.
 ———. 2013. “ANSYS Fluent Theory Guide,” no. November: 591.
 Banerjee, D., and V. K. Dhir. 2001. “Study of Subcooled Film Boiling on a Horizontal Disc: Part I—Analysis.” *Journal of Heat Transfer* 123 (2): 271–84. doi:10.1115/1.1345889.
 Berenson, P. J. 1961. “Film-Boiling Heat Transfer From a Horizontal Surface.” *Journal of Heat Transfer*, 351–56.
 Brackbill, J. U., D. B. Kothe, and C. Zemach. 1992. “A Continuum Method for Modeling Surface Tension.” *Journal of Computational Physics* 100: 335–54.
 Carey, V.P. 1992. *Liquid-Vapor Phase Change Phenomena: An Introduction to the Thermophysics of Vaporization and Condensation Process in Heat Transfer Equipment*. Washington ,D.C.: Hemisphere Publishing Corp.
 Dhir, Vijay K. 2001. “Numerical Simulations of Pool-Boiling Heat Transfer.” *AICHE Journal* 47 (4): 813–34. doi:10.1002/aic.690470407.
 Esmaeeli, Asghar, and Grétar Tryggvason. 2004. “Computations of Film Boiling. Part I: Numerical Method.” *International Journal of Heat and Mass Transfer* 47 (25): 5451–61. doi:10.1016/j.ijheatmasstransfer.2004.07.027.
 Juric, Damir, and Gretar Tryggvason. 1998. “Computations of Boiling Flows.” *International Journal of Multiphase Flow* 24 (3): 387–410.
 Klimenko, V. V. 1981. “Film Boiling on a Horizontal Plate - New Correlation.” *International Journal of Heat and Mass Transfer* 24 (1): 69–79. doi:10.1016/0017-9310(81)90094-6.
 Liu, Yi, Tomasz Olewski, Luc Vechot, Xiaodan Gao, and Sam Mannan. 2011. “Modelling of a Cryogenic Liquid Pool Boiling Using CFD Code.” In *14th Annual Symposium, Mary Kay O’Connor Process Safety Center*.
 Merte, H., and J.A. Clark. 1964. “Boiling Heat Transfer With Cryogenic Fluids at Standard , Fractional and Near-Zero Gravity.” *Journal of Heat Transfer* 86 (3): 351–58.
 Rowley, R.L., W.V. Wilding, J.L. Oscarson, J.L. Zundel, N.A. Marshall, T. L. Daubert, and R.P. Danner. 2003. *DIPPR Data Compilation of Pure Compound Properties*. Design Institute for Physical Property Data/AICHE.
 Sernas, V., J. H. Lienhard, and Vijay K. Dhir. 1973. “The Taylor Wave Configuration During Boiling from a Falt Plate.” *International Journal of Heat and Mass Transfer* 16: 1820–21.
 Son, G., and V. K. Dhir. 1997. “Numerical Simulation of Saturated Film Boiling on a Horizontal Surface.” *Journal of Heat Transfer* 119 (August 1997): 525–33.
 Son, G., and Vijay K. Dhir. 1998. “Numerical Simulation of Film Boiling Near Critical Pressures With a Level Set Method.” *Journal of Heat Transfer* 120 (February): 183–92.
 Tomar, G., G. Biswas, a. Sharma, and a. Agrawal. 2005. “Numerical Simulation of Bubble Growth in Film Boiling Using a Coupled Level-Set and Volume-of-Fluid Method.” *Physics of Fluids* 17 (11): 112103. doi:10.1063/1.2136357.

- Véchet, Luc, Tomasz Olewski, Carmen Osorio, Omar Basha, Yi Liu, and Sam Mannan. 2013. "Laboratory Scale Analysis of the Influence of Different Heat Transfer Mechanisms on Liquid Nitrogen Vaporization Rate." *Journal of Loss Prevention in the Process Industries* 26 (3). Elsevier Ltd: 398–409. doi:10.1016/j.jlp.2012.07.019.
- Webber, D M, S E Gant, M J Ivings, and S F Jagger. 2010. *LNG Source Term Models for Hazard Analysis: A Review of the State-of-the-Art and an Approach to Model Assessment*. Research Report: RR789. HSE Books. Buxton, Derbyshire, UK. <http://www.hse.gov.uk/research/rrpdf/rr789.pdf>.
- Welch, Samuel W. J., and Thami Rachidi. 2002. "Numerical Computation of Film Boiling Including Conjugate Heat Transfer." *Numerical Heat Transfer, Part B* 42: 35–53.
- Welch, Samuel W. J., and John Wilson. 2000. "A Volume of Fluid Based Method for Fluid Flows with Phase Change." *Journal of Computational Physics* 160 (2): 662–82. doi:10.1006/jcph.2000.6481.
- Youngs, D. L. 1982. "Time Dependent Multi-Material Flow with Large Fluid Distortion." In *Numerical Methods in Fluid Dynamics*, edited by K.W. Morton and M.J. Baines, 273–85. Academic Press.
- Yuan, M.H., Y.H. Yang, T.S. Li, and Z.H. Hu. 2008. "Numerical Simulation of Film Boiling on a Sphere with a Volume of Fluid Interface Tracking Method." *International Journal of Heat and Mass Transfer* 51 (7-8): 1646–57. doi:10.1016/j.ijheatmasstransfer.2007.07.037.
- Zuber, Novak. 1959. "Hydrodynamic Aspects of Boiling Heat Transfer." University of California, Los Angeles.